Substrate Integrated Waveguide-Based Periodic Backward-to-Forward Scanning Leaky-Wave Antenna With Low Cross-Polarization

Debabrata K. Karmokar, *Member, IEEE*, Y. Jay Guo, *Fellow, IEEE*, Pei-Yuan Qin, *Member, IEEE*, Shu-Lin Chen, *Student Member, IEEE*, and Trevor S. Bird, *Life Fellow, IEEE*

***Abstract*— For many leaky-wave antennas (LWAs), it is challenging to realize beam scanning through broadside. A problem is the presence of an open stopband (OSB), which restricts radiation in the broadside direction. In this paper, a novel substrate integrated waveguide (SIW)-based LWA is described to overcome the OSB problem and provide beam scanning continuously from the backward to the forward direction from a conventional periodic LWA. It is demonstrated that the $n = -1$ spatial harmonic can be excited efficiently from an SIW LWA and enables broadside radiation. However, it was found in our initial design that when the beam scans through the broadside, the cross-polarization level increases significantly compared to the beam close to the backfire direction. A technique is developed to reduce the cross-polarization level. As a result, a new antenna configuration is created. The antenna design has been realized and measured to validate the concept. The measured beam scanning range of the prototype is from -74° to $+45^\circ$ (119° of beam scanning) when the frequency sweeps from 7.625 to 11 GHz, and the measured cross-polarization level is 20.8 dB low at the main beam direction for the broadside beam.**

***Index Terms*— Backward-to-forward scanning, beam scanning, broadside beam, leaky-wave antenna (LWA), open stopband (OSB), substrate integrated waveguides (SIWs).**

I. Introduction

LEAKY-wave antennas (LWAs) are popular due to their inherent beam scanning capabilities with frequency [1]–[3]. They can be an excellent candidate for various applications where wide range antenna beam scanning is required, such as for frequency scanning radars and surveillance [3], [4]. LWAs have been known since the 1940s through the studies based on waveguides [5]. Since then, various studies have been conducted on waveguide-based LWAs [6]–[10]. Microstrip-based LWAs were developed in the late 1970s [11], [12]. Following this, they gained a significant research interest and their modes of operation were investigated in detail [13]–[15]. The substrate integrated waveguide (SIW) is another attractive technology in microwave engineering, as the bulky and costly waveguide can be replaced by a planar microstrip technology. Due to their planar low-profile configuration, SIWs are used in different types of antenna designs, especially in LWAs. LWAs based on microstrip technology are suitable to be integrated with millimeter-wave and microwave circuits [16], [17].

Several types of LWAs have been proposed so far for beam scanning. Most uniform and periodic unidirectional LWAs scan the beam in the forward direction only. For example, an LWA proposed in [18] uses transverse slots on the microstrip, which enables the antenna to scan in the forward direction with improved radiation toward the endfire. A butterfly SIW LWA was proposed in [19], which scans the main beam in the forward direction as well. An SIW-based LWA proposed in [20] radiates from a long slot in the broad wall. The beam of the antenna also scans in the forward direction. There are other different types of forward beam scanning SIW-based LWAs such as a half-mode SIW LWA [21]. Some other periodic LWAs offer multiband operation and are also able to scan the main beam in both the backward and forward directions, but are unable to scan the beam through broadside without significant gain losses [16], [22]. Very limited study has been conducted on conventional periodic LWAs for beam scanning through the broadside direction.

Some studies have been conducted to achieve a broadside beam from uniform or periodic LWAs. To do this, several uniform or periodic LWAs are formed into a radial array and these arrays are usually unable to scan the main beam separately, since the individual beams of the LWAs are combined together to produce a broadside beam [23]–[26]. Some other LWA structures have both the left and right-handed properties, called composite right/left handed that enable the beam to be scanned through the broadside direction under the balanced condition [27]–[31].

The inability to continuously beam scan through the broadside remains a significant drawback for the conventional unidirectional periodic LWA structures. This is because, for most cases, the traveling wave LWA turns into a standing-wave antenna at the broadside scanning frequency, and the open stopband (OSB) restricts the broadside radiation [1]. To achieve a broadside beam from a conventional LWA has

Manuscript received August 12, 2017; revised February 20, 2018; accepted April 17, 2018. Date of publication May 11, 2018; date of current version August 2, 2018. This work was supported by Australian Research Council under Discovery Project 160102219. *(Corresponding author: Debabrata K. Karmokar.)*

The authors are with the Global Big Data Technologies Centre, University of Technology Sydney, Ultimo, NSW 2007, Australia (e-mail: dkkarmokar@ieee.org; jay.guo@uts.edu.au; peiyuan.qin@uts.edu.au; shulin.chen@uts.edu.au; ts.bird@ieee.org).

Color versions of one or more of the figures in this paper are available online at http://ieeexplore.ieee.org.

Digital Object Identifier 10.1109/TAP.2018.2835502

been of a significant research interest [32], [33]. Different types of unidirectional periodic LWAs have been investigated so far to achieve continuous beam scanning from backward to forward directions through broadside. Some periodic half-width microstrip LWAs are proposed to achieve continuous backward-to-forward beam scanning by changing the placement of shorting vias [34], [35]. However, the radiated beam degrades significantly when it points near or toward the broadside direction. Two LWAs have been proposed recently to achieve a continuous beam scan from backward to forward direction through broadside. By using longitudinal and transverse slots in an SIW, the OSB was suppressed and continuous beam scanning is achieved [36]. An LWA based on a dielectric image line has been proposed for the same purpose [37].

In this paper, we propose a new class of SIW-based LWAs to overcome the OSB problem of unidirectional periodic LWAs to scan the beam through the broadside direction. These new LWAs can scan the beam continuously from backward to forward direction. It was found that when the antenna scans from backward to forward direction, the cross-polarization increases significantly. A technique has been developed to reduce the cross-polarization level throughout the scanning range. Finally, one antenna design is realized and tested, and the measured results validate the concept of the new antenna design.

II. Beam Scanning From Periodic LWA

The direction of the main beam of an LWA is a function of frequency, and for each frequency point, it is determined by the phase constant (β) and free-space wavenumber (k_0) [16]. In the case of a periodic LWA, the phase constant depends on the period P of the structure. For the n^{th} periodic mode, the phase constant is expressed in [17]

$$\beta_n = \beta_0 + n\frac{2\pi}{P} \tag{1}$$

where β_0 is the space harmonic for the fundamental mode.

To achieve a single beam radiating from backward to forward direction, $n = -1$ space harmonic is needed [17], so that (1) can be written as

$$\beta_{-1} = \beta_0 - \frac{2\pi}{P} \tag{2}$$

For a periodic LWA radiating the $n = -1$ space harmonic, the direction of the main beam is given as

$$\theta(f) \approx \sin^{-1}\left[\frac{\beta_{-1}(f)}{k_0(f)}\right] \tag{3}$$

where θ is the angle measured from the broadside [17]. It can be seen from (3) that β_{-1}/k_0 varies as does the beam direction with frequency. The main beam (radiation of $n = -1$ space harmonic) points close to the backfire direction at low frequencies and scans toward broadside as the frequency increases. When the main beam points toward the broadside direction, i.e., $\theta = 0^\circ$ in (3), $\beta_{-1} = 0$ then (2) gives

$$\beta_0 = \frac{2\pi}{\lambda_g} = \frac{2\pi}{P} \tag{4}$$

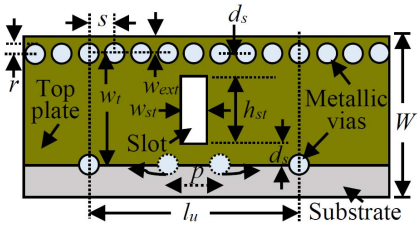

Fig. 1. Unit cell design to achieve continuous beam scanning from backward to forward direction through broadside. The schematic shown here is not to scale.

where λ_g is the guided wavelength of a structure. From (4), we see that for continuous beam scanning through broadside, the period P should be equal to λ_g.

In the case of conventional periodic LWAs, there is a significant drop of radiation in the OSB region due to the reflection of power to the source instead of radiation [38]. To achieve continuous beam scanning from backward to forward direction, two conditions need to be satisfied simultaneously. First, the phase constant β_{-1} should vary linearly, i.e., without any bandgap. Second, the power leakage should not change rapidly. The OSB in the broadside radiation can be suppressed by utilizing a reflection canceling unit cell or by designing a unit cell with an impedance matching transformer in it [39], [40]. In Section III, the design of a unit cell is discussed following the requirement to suppress the OSB.

III. Unit Cell Design to Overcome Open Stopband

To overcome the OSB problem, we conduct our analysis on a unit cell (the schematic is shown in Fig. 1) design first. A 1.575 mm thick Rogers RT5870 substrate is used for the unit cell design. The dielectric constant (ε_r) of the substrate is 2.33. An impedance matching technique is used in our unit cell design for broadside radiation. A smooth transition between the backward and forward directions without significant degradation of the broadside radiation is achieved by ensuring appropriate power leakage as well as controlling the phase constant simultaneously. To ensure leakage for the broadside beam, initially, a transverse slot was allowed on the top plate of each unit cell to leak power similar to the conventional SIW-based LWAs. Both edges of the top plate are shorted to the ground plane by a closely placed array of vias as shown in the upper edge of Fig. 1. The upper edge of the top plate is aligned with the edge of the substrate which is 1.4 mm away ($w_{\text{ext}} = 1.4$ mm) from the center of the via array. However, the lower edge of the top plate is aligned with the center of the via as shown in Fig. 1 to achieve more leakage from the structure. The radius (r) of the via is 0.4 mm and the center-to-center distance (s) between two vias is 2 mm. There is a negligible leakage from the upper via wall due to the very close spacing ($s/2r = 2.5$ and $2r/w_t \approx 0.05$). The propagation constant of an SIW-based LWA can be controlled by controlling the distance between two adjacent vias [17], [41]. In order to achieve the $n = -1$ spatial harmonic radiation, the distance (P) between two vias in the lower edge was used to study the leakage and its effect on the beam direction. In our study, a parametric analysis is used to find the optimum distance P between two vias in the lateral

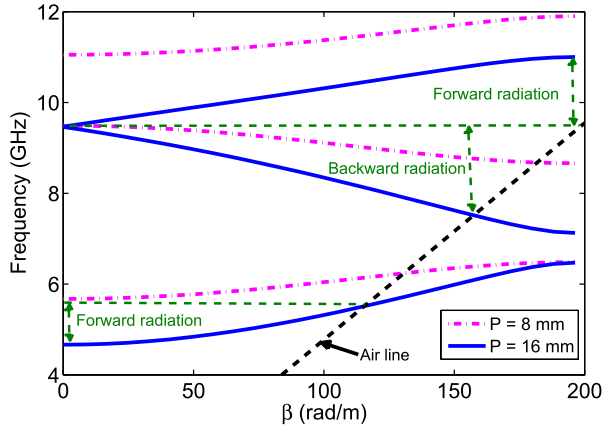

Fig. 2. Dispersion diagram of the unit cell shown in Fig. 1 for two different values of the distance (P) between lower vias.

SIW wall to suppress the bandgap. This study was undertaken using the CST Microwave Studio eigenmode solver to observe the phase constant, and the radiation property of the unit cell is observed through full-wave simulation by using it in a finite structure as discussed in Section IV. It was found that by choosing appropriate dimensions of a unit cell, the impedance could be matched in the broadside radiation, i.e., the OSB can be suppressed completely and good radiation was achieved.

With an increase in the distance between the two lower vias, the bandgap at $\beta_{-1} = 0$ rad/m between the higher two modes decreases. The dispersion diagrams for two different values of P are shown in Fig. 2. When increasing the distance P between the two vias in the lateral SIW wall, it was found that for a particular value of P (16 mm for the current design), the bandgap suppresses completely, indicating continuous beam scanning through broadside ($\beta = 0$ rad/m) from the upper two modes. The radiation properties in the lower band (fundamental mode) are similar to conventional SIW-based LWAs, i.e., forward beam scanning. It is well known from the previous study as well was verified by our analysis that in the fundamental mode the main beam points in the forward direction. As mentioned before, when the power radiates from a structure due to the $n = -1$ spatial harmonic, the beam points in the backward direction at low frequencies move toward the broadside direction and then move in the forward direction with an increasing frequency (see Fig. 2).

The dimensions of the final unit cell are: the slot is located at the center of the top plate and it is 2.125 mm away from the center of the vias, i.e., $d_s = 2.125$ mm. The length (l_u) of the unit cell, the width (W) of the substrate, and the width (w_t) of the top plate are 16, 18.8, and 16 mm, respectively. The dimensions of the slot are 11.75 mm $\times$ 3 mm ($h_{\rm st} \times w_{\rm st}$), where $h_{\rm st}$ and $w_{\rm st}$ are the height and width of the slot, respectively.

A complete finite structure was then designed using the unit cell to observe the antenna performance in the continuous beam scanning band and this will be described in Section IV.

IV. Complete Antenna Design for Continuous Beam Scanning

A complete finite SIW-based LWA is designed in this section using the unit cell approach outlined in Section III to study the performance of the unit cell in a finite antenna design. The antenna design and the detailed investigations are given in Sections IV-A–IV-C. As will become clearer later, to assist the discussion easy, we refer to this antenna as LWA1.

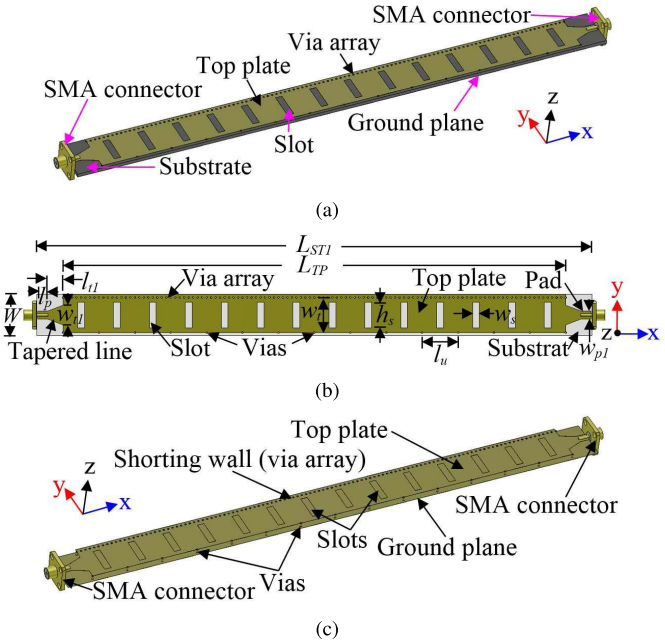

Fig. 3. Complete antenna design (LWA1) using the unit cell investigated in Section III to get beam scanning from backward to forward direction. (a) 3-D view. (b) Top view with detailed geometric parameters. (c) Perspective view (substrate omitted).

A. Antenna Configuration

Fig. 3 shows the configuration of the antenna (LWA1) designed using the unit cell analyzed in Section III to achieve continuous beam scanning. Fig. 3(a)–(c) shows the 3-D view, top view with detailed geometric parameters, and perspective view (omitting the substrate) of the antenna. The antenna consists of 14 unit cells which makes the length ($L_{\rm TP}$) of the top plate 224 mm ($7.08\lambda_0$ at 9.48 GHz). As mentioned in Section III, one edge [upper edge in Fig. 3(b)] of the top plate is shorted to the ground plane by a closely placed array of vias. The other edge [lower edge in Fig. 3(b)] of the top plate is partially shorted to the ground plane by two vias, one at each end of a unit cell. The antenna is fed from one side [Fig. 3(a) (left)] and the other side is terminated in a 50 Ω load. There is a small patch called a "pad" is placed at each side of the antenna to connect the SMA connector inner conductor. The length (l_p) of the pad is chosen based on the length of the SMA connector inner conductor, and the width (w_p) of the pad was obtained using parameter analysis to get the best input impedance matching.

For improved impedance matching, a tapered line is used between the matching pad and the top plate. The dimensions of the tapered line were optimized using parameter analyses conducted with the software package CST Microwave Studio. The length (l_t) of the tapered line is 7 mm. The width (w_{t1}) of the final tapered line at the top plate end and the width (w_{p1})

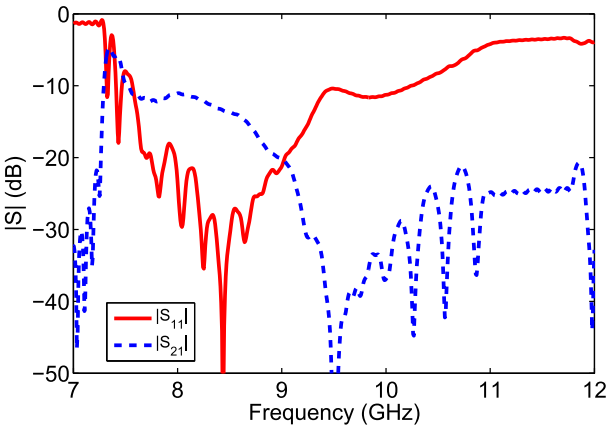

Fig. 4. Predicted scattering parameters of the transverse slot loaded SIW-based LWA1 in Fig 3.

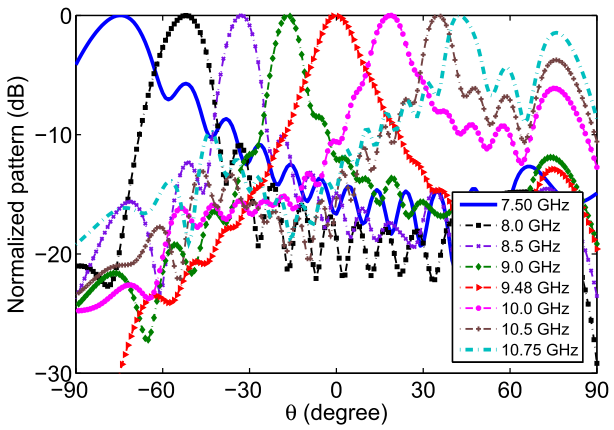

Fig. 5. Predicted normalized radiation patterns (xz plane) of the transverse slot-loaded SIW-based LWA1 in Fig 3.

at the pad end are 9 and 3.7 mm, respectively. The width (w_{p1}) of the pad is the same as that of the tapered line at the pad end, and the length (l_p) of the pad is 4.5 mm. There is a small 0.5 mm gap between the pad and the edge of the substrate to avoid any unwanted electrical connection between the SMA inner and outer conductors during soldering in the actual prototype. It is worth mentioning that in the current antenna design, our main focus is continuous beam scanning from backward to forward direction, and hence, all the analyses are conducted accordingly. Following the optimization and design, the overall length (L_{ST1}) and width (W) of the LWA structure are 248 and 18.8 mm, respectively.

B. S-Parameters

The antenna was analyzed using CST Microwave Studio. Fig. 4 shows the predicted scattering parameters of the antenna geometry shown in Fig. 3. The antenna has a -10 dB reflection bandwidth from 7.57 to 10.24 GHz. The reflection coefficient at 9.48 GHz is -10.4 dB, where the transition occurs, i.e., the frequency point where the main beam points in the broadside direction. Between 9.24 and 10.75 GHz, the reflection coefficient remains <-6.26 dB. The transmission $|S_{21}|$ is high at lower frequencies and decreases gradually as the frequency increases. For example, at 7.5 GHz, the transmission coefficient is -9.62 dB, while at 9 GHz, it drops to -20.1 dB. The simultaneous low reflection and transmission coefficients on the structure indicate an excellent radiation performance of the antenna.

C. Radiation Patterns

The predicted normalized radiation patterns of the antenna are shown in Fig. 5. Similar to the conventional 1-D LWA, the antenna produces a fan-shaped beam, where the beamwidth is wider in the yz plane and narrower in the xz plane. The antenna scans the beam continuously from $-75°$ to $+42°$ on the xz plane with a frequency sweep from 7.5 to 10.75 GHz. The gain of the antenna is >10 dBi within a scan range of $-75°$–$+35°$. However, the gain falls to 8.7 dBi for beam angles $> +42°$. This occurs because of the poor impedance matching at high frequency and increasing sidelobes as shown in Fig. 5.

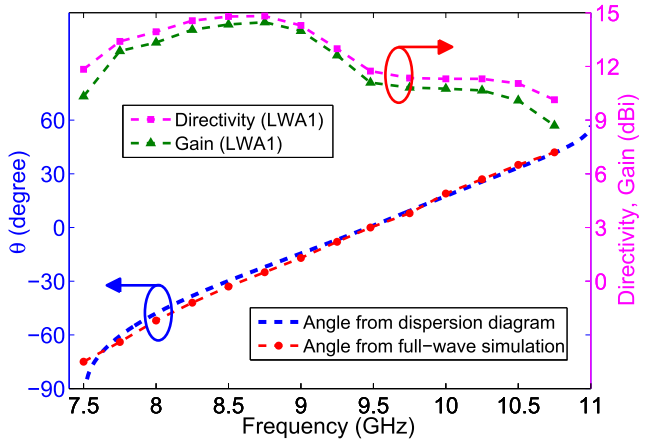

Fig. 6. Comparison of angle predicted from dispersion diagram in Fig. 2 and from CST full-wave simulation of the LWA1 in Fig. 3, and predicted gain and directivity of the same antenna. There are 14 unit cells in LWA1.

The present antenna design is polarized in the x-direction. It was found that when the main beam scans close to the backfire direction (backward endfire), the cross-polarization is low. However, as the beam moves close to the broadside direction, the cross-polarization level increases. At the transition, i.e., at broadside, the amplitude of the cross-polarization is very high and it remains high beyond broadside as the beam scans in the forward direction. In order to reduce the cross-polarization level at different beam positions, investigations on the antenna structure were conducted and a detailed discussion follows in the later sections.

Fig. 6 shows the beam direction calculated from the dispersion diagram in Fig. 2, using (3), compared with the angles predicted by a full-wave simulation of the complete structure in Fig. 3 using CST Microwave Studio. Excellent agreement is observed between the two results. The slight variation between two results at the bottom and top of the band is as anticipated, as the dispersion diagram shows the characteristics of a structure with an infinite number of unit cells. However, the finite antenna structure in Fig. 3 consists of only 14 unit cells. The predicted gain and directivity of LWA1 are also given in Fig. 6 to show the radiation property of the antenna at

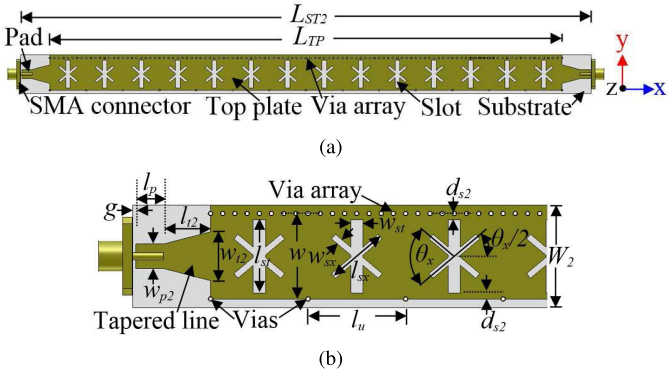

Fig. 7. SIW-based LWA (LWA2) with combined transverse and cross-shaped slots. (a) Top view. (b) Details of feed section, slot dimensions, and unit cell.

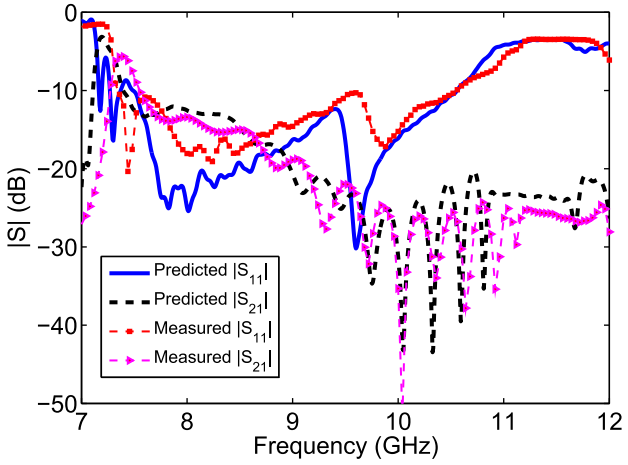

Fig. 8. Predicted (antenna in Fig. 7) and measured (prototype in Fig 15) S-parameters of LWA2.

different beam directions. It can be observed that the antenna has good radiation characteristics throughout the beam scan range.

V. Antenna Design to Reduce the Cross-Polarization Level

It is observed in Section IV that the cross-polarization increases significantly when the beam scans close to broadside and beyond it into the forward direction. This is the main problem with an LWA that is designed using a unit cell containing a transverse slot at its center. This is because the radiation from the transverse slot is polarized in the x-direction, whereas radiation from the lateral SIW wall is polarized in the y-direction. As discussed in Sections II and III, a separation (P for the current design) is required between two vias in the lateral SIW wall together with a slot on the top plate to suppress the OSB. So, an effective way is necessary to reduce the cross-polarization while maintaining the distance P. To minimize the cross-polarization, we added a cross ($\times$)-shaped slot with the transverse slot. An antenna design using combined transverse and cross-shaped slots is described as follows, which we shall refer to as LWA2. The radiation mechanism is further explained in Section VI-A.

A. Antenna Configuration

The configuration of this new antenna design LWA2 is shown in Fig. 7. Since a new type of slot is used in the unit cell, the dimensions of the unit cell have been optimized, maintaining the length of the unit cell the same, to achieve a similar range of impedance bandwidth as of LWA1. The top view of the new antenna design is shown in Fig. 7(a), and Fig. 7(b) shows the parameters in detail. The dimensions of the new slot were optimized to obtain good radiation and matching. The dimensions of the transverse slot are 12 mm $\times$ 2 mm ($l_{\rm st} \times w_{\rm st}$), where $l_{\rm st}$ and $w_{\rm st}$ are the length and width of the slot, respectively. Similar to the first design LWA1, the slot is at the center of the unit cell, leaving a distance (d_{s2}) of 1 mm from the lower edge of the top plate. The center of the cross-shaped slot is aligned with the center of the transverse slot. The length ($l_{\rm sx}$) and width ($w_{\rm sx}$) of each branch of the cross-shaped slot are 10 and 1 mm, respectively. The width of the substrate (W_2) and the top plate (w) are 16.8 and 14 mm, respectively. Introduction of this new slot in the antenna design changes the input impedance of the antenna. In order to improve the impedance match, the parameters of the matching section need to be reoptimized. Parametric analyses were conducted to get the optimum dimensions of the tapered line and the pad. The optimized length l_{t2} is 7.75 mm and the width w_{t2} of the tapered line at the top plate end is 8 mm. The optimized width w_{p2} of the pad is 4 mm. The overall length $L_{\rm ST2}$ of the new antenna structure is 249.5 mm.

To observe the antenna performance for the beam at broadside, we investigated the angle between the cross arms, i.e., the dual slot is modified maintaining the antenna configuration the same. It was found that when the angle (θ_x) between the cross arms reduces, it also reduces the cross-polarization level for the broadside beam. However, the directivity and gain of the antenna deteriorate slightly (discussed later) with the angle of the cross branch. An angle θ_x of 80° was chosen between the cross-shaped slot branches in terms of the cross-polarization level and the directivity of the antenna. So, the angle ($\theta_x/2$) between a branch and the x-axis is 40°.

B. Antenna Performance

Fig. 8 shows the predicted S-parameters of the antenna in Fig. 7. The −10 dB reflection bandwidth covers a frequency range from 7.49 to 10.56 GHz. The reflection coefficient is greater than −10 dB beyond 10.56 GHz, but it remains below −7.1 dB up to 10.75 GHz. The $|S_{11}|$ below frequency 7.49 GHz is greater than −10 dB but remains below −8.68 dB until 7.35 GHz. It can be seen that the impedance bandwidth is slightly wider compared to LWA1. Similar to the antenna with transverse slots (LWA1), the predicted transmission is high at lower frequencies and decreases with frequency. For example, the transmission at 7.5 and 9.5 GHz are −12.5 and −24.3 dB, respectively, indicating a very good radiation property.

Fig. 9 shows the predicted xz plane radiation patterns (normalized) of LWA2. The antenna has a beam scanning range from −75° to +46° when the frequency sweeps from 7.35 to 10.75 GHz. The beam scanning range of LWA2 is slightly larger than that of LWA1. It can be seen from Fig. 10

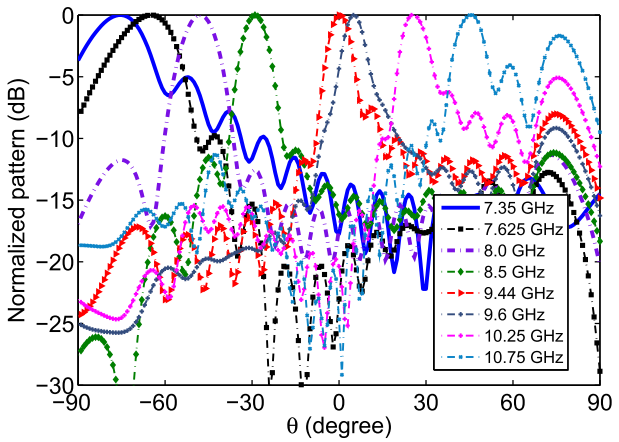

Fig. 9. Predicted normalized radiation patterns (xz plane) of the SIW-based LWA2 (with $\theta_x = 80°$) shown in Fig 7.

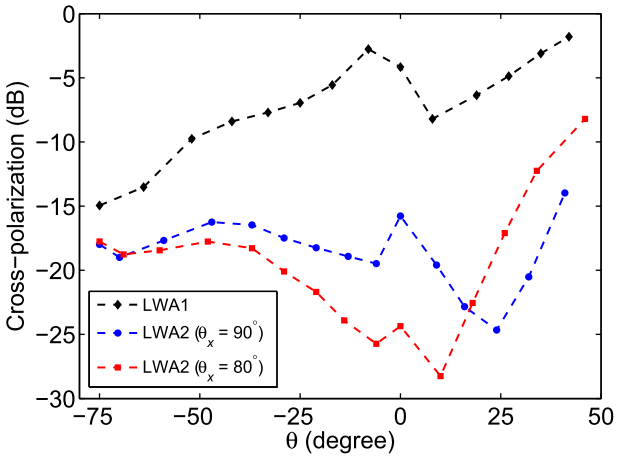

Fig. 10. Predicted cross-polarization level of LWA1 and LWA2 with respect to normalized co-polarization level.

that the cross-polarization level of LWA2 reduces significantly throughout the beam scanning range. When comparing the performance of LWA2 for different values of θ_x, the cross-polarization level is lower over a wider scanning range for $\theta_x = 80°$ than for $\theta_x = 90°$. However, the cross-polarization is greater for some beam directions in the forward direction than the latter.

The performance of the LWAs is described further in Section VI.

VI. Performance Comparison of the Backward-to-Forward Beam Scanning SIW LWAs

A. Cross-Polarization Level

The cross-polarization levels of both LWAs investigated in this paper are shown in Fig. 10 at different beam positions. The cross-polarization level was taken at the beam direction (normalized) on the xz plane. It can be seen from Fig. 10 that the cross-polarization level is low when the main beam points close to the backfire direction. For example, the cross-polarization level of LWA1, LWA2 with $\theta_x = 90°$, and LWA2 with $\theta_x = 80°$ are -14.95, -17.99, and -17.76 dB, respectively, when the main beam points at $-75°$. However, the cross-polarization level increases significantly for LWA1 when the main beam approaches the broadside direction. For example, the cross-polarization level is only -2.77 dB when the main beam points at $-8°$. The cross-polarization level decreases slightly when the beam scans at the forward direction and then increases and reaches -1.8 dB at $+42°$. In the case of LWA2, the cross-polarization level is ≤ -14 dB throughout the scanning range when $\theta_x = 90°$. The cross-polarization level of LWA2 for $\theta_x = 80°$ is lower for most of the scanning region than for $\theta_x = 90°$. For example, the cross-polarization level for the broadside beam of LWA2 with $\theta_x = 90°$ and $\theta_x = 80°$ are -15.8 and -24.4 dB, respectively. However, the cross-polarization for $\theta_x = 80°$ is greater than for $\theta_x = 90°$ in some forward beam directions as shown in Fig. 10.

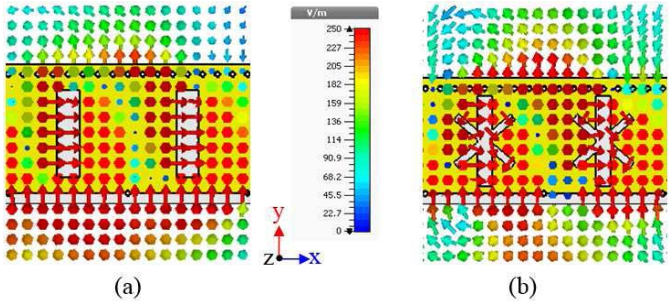

Fig. 11. Electric field on the top surface. (a) LWA1. (b) LWA2 with $\theta_x = 80°$. A short section is shown here for better representation of the field.

Fig. 11 shows the electric field distribution on the top (xy plane) of the antenna structure when the main beam points at the broadside direction. In the case of LWA1 [Fig. 11(a)], it is clear that the antenna radiates from the transverse slot at the center of the unit cell which is polarized in the x-direction. Radiation also occurs from the lateral SIW wall which is polarized in the y-direction. This is the main reason for the high cross-polarization level when the main beam scans through the broadside direction. However, for LWA2 [Fig. 11(b)], the radiation from the dual slot has two components. The radiation from the transverse slot is polarized in the x-direction and the radiation from the cross-shaped slot is polarized in the y-direction and is phased opposite to the radiation from the lateral SIW wall. The two field components (from lateral SIW wall and cross slot) cancel each other and a nearly pure polarization field is achieved in the main beam direction.

B. Antenna Efficiency

The predicted radiation and total efficiencies of both the antennas are shown in Fig. 12. The radiation efficiency of LWA1 is greater than 84% throughout the band (7.5–10.75 GHz) and is greater than 90% beyond 8.5 GHz. The total efficiency of the antenna is >70% throughout the scanning range. The total efficiency of the antenna remains >85% between 7.7 and 10.25 GHz. The total efficiency drops

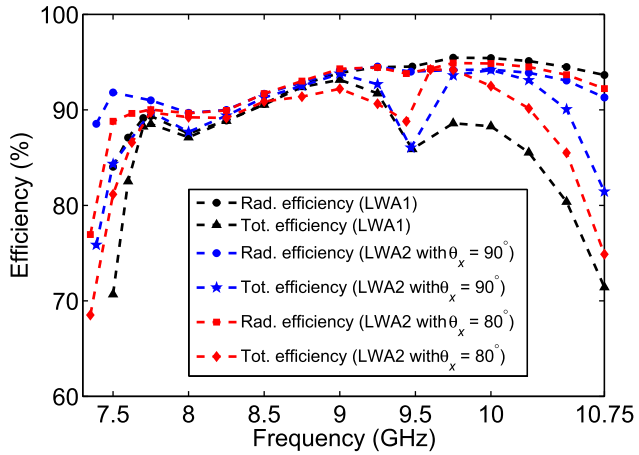

Fig. 12. Predicted radiation and total efficiencies of LWA1 and LWA2.

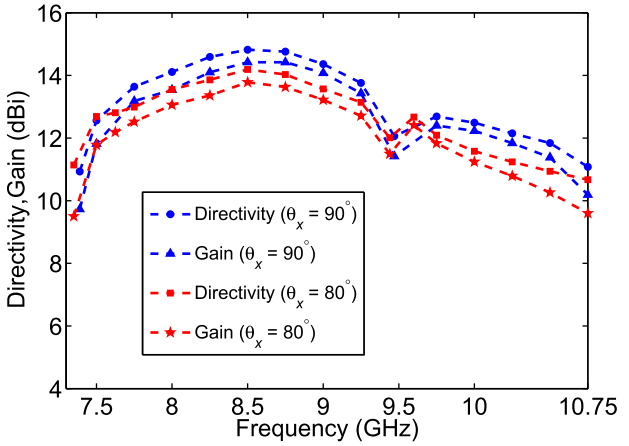

Fig. 13. Predicted directivity and gain of LWA2 for two different angles (θ_x) between the cross arms.

at frequencies >10.25 GHz due to poor impedance matching of the antenna at higher frequencies. This happens because the total efficiency considers the impedance mismatch loss. However, the radiation efficiency is the ratio of the radiated power to the power delivered to the antenna. The radiation efficiency of LWA2 with $\theta_x = 90°$ is >88% throughout the scanning range and the total efficiency of the antenna is above 81% throughout the band except at the lower frequency point where the reflection coefficient is above −10 dB. With $\theta_x = 80°$, the radiation efficiency is >89% within the frequency range beyond 7.5 GHz, but the radiation efficiency at 7.35 GHz is 77%. The total efficiency of the antenna is >85% at most of the frequency points except at lower and higher frequency points as shown in Fig. 12, which is mainly due to an impedance mismatch at these frequency points. From the efficiency curves, it can be seen that the antennas have excellent radiation performance throughout the frequency band. It is worth emphasizing here that the radiation efficiency of most conventional uniform and some periodic LWAs drops significantly when the main beam scans away from the broadside direction, i.e., as the scanning angle increases.

TABLE I
COMPARISON BETWEEN THE SIW-BASED LWAS

Antenna	Cross-Polarization	Broadside Gain	Scanning Range
LWA1	−2.8 dB	11.10 dBi	−75° to +42°
LWA2 ($\theta_x = 90°$)	−15.8 dB	11.40 dBi	−75° to +41°
LWA2 ($\theta_x = 80°$)	−24.4 dB	11.50 dBi	−75° to +46°
LWA2 prototype	−20.8 dB	10.60 dBi	−74° to +45°

The cross-polarization levels listed here are for the broadside beam.

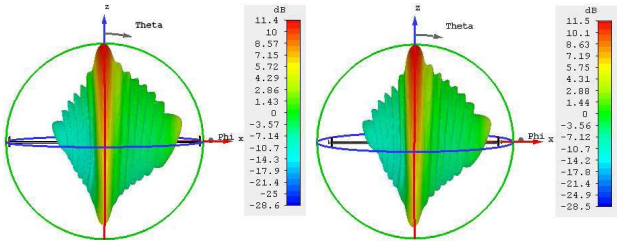

(a) (b)

Fig. 14. 3-D radiation (gain) patterns when the main beam points toward the broadside direction. (a) LWA2 with $\theta_x = 90°$. (b) LWA2 with $\theta_x = 80°$.

C. Gain and Directivity

The predicted directivity and gain of LWA2 for two different angles (θ_x) between the cross arms are illustrated in Fig. 13. The directivities and, hence, the gains are low at lower frequencies for both the cases. For example, the directivity and gain at 7.75 GHz are 13 and 12.52 dBi, respectively, for LWA2 with $\theta_x = 80°$. The gain and directivity increase with frequency (directivity and gain are 14.2 and 13.8 dBi, respectively, at 8.5 GHz). The directivity and gain reduce as the main beam moves toward the broadside. However, they increase slightly when the frequency increases, i.e., the main beam points away from the broadside and then drops again. With $\theta_x = 90°$, the directivity and gain curves are similar to those with $\theta_x = 80°$; however, their values are slightly larger than those of LWA2 with $\theta_x = 80°$. For example, the gain and directivity at 7.75 GHz are 13.2 and 13.64 dBi, respectively, with $\theta_x = 90°$. The gains for the beam at broadside are 11.4 and 11.5 dBi, respectively, for $\theta_x = 90°$ and $\theta_x = 80°$. For LWA1, the gain and directivity are high when the beam scans in the backward direction (shown in Fig. 6), but they drop significantly when the main beam scans in the forward direction. The 3-D gain patterns of LWA2 for two different θ_x are shown in Fig. 14, when the main beam points in the broadside direction.

The performance of both the antennas in terms of the cross-polarization level of the broadside beam, broadside gain, and scanning range are listed in Table I. Results in the first three rows of Table I corresponding to LWA1, LWA2 ($\theta_x = 90°$), and LWA2 ($\theta_x = 80°$) are predicted results, and Section VII describes the measured results that are also listed.

VII. MEASURED RESULTS

To prove the concept for the present antennas, one of the earlier designs was fabricated and tested. Taking into account

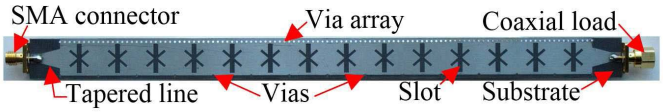

Fig. 15. Photograph of the fabricated prototype (LWA2 with $\theta_x = 80°$).

the impedance matching and scanning range, LWA2 with $\theta_x = 80°$ was fabricated and measured. A photograph of the fabricated antenna is shown in Fig. 15. As mentioned earlier, the LWA is fed from one side (left SMA connector in Fig. 15) and the other side is terminated in a 50 Ω load (the right SMA connector is terminated in 50 Ω load). This section discusses the performance of the prototype antenna in terms of the impedance bandwidth, radiation patterns, and gain.

A. S-Parameters

The measured reflection coefficient and the transmission of LWA2 with $\theta_x = 80°$ are shown in Fig. 8. The S-parameters of the prototype were measured using a KEYSIGHT PNA-N5225A network analyzer. A very good agreement is observed between the measured and predicted results. There is a slight difference between the predicted and measured S-parameters, as the measured reflection coefficient curve is marginally shifted higher in frequencies. This may occur due to minor fabrication errors. The prototype has a −10 dB reflection coefficient bandwidth from 7.36 to 10.52 GHz. Beyond 10.52 GHz, the reflection coefficient is higher than −10 dB and it gradually increases. For example, the reflection coefficients at 10.75 and 11 GHz are −8.2 and −5.74 dB, respectively. The measured transmission of the antenna is high at lower frequencies and it decreases with frequency. The measured transmission at 7.52 GHz is −8.94 dB. The transmission coefficient of the antenna remains <-20 dB beyond 9.16 GHz.

B. Radiation Patterns

The measured normalized xz plane radiation patterns of the LWA2 prototype are shown in Fig 16. The beam scans from −74° to +45° when the frequency sweeps from 7.625 to 11 GHz. A beam scanning range of 119° is achieved from the measurement. As the frequency increases, the beam moves from close to backfire (−74°) toward the broadside direction (at 9.6 GHz), then it scans in the forward direction and points at +45° at 11 GHz. The cross-polarization level is low throughout the scanning range except for the beam which points away from broadside in the forward direction. For example, the measured cross-polarization level for the beam at −31° (8.5 GHz) and +45° (11 GHz) are −19.5 and −8.6 dB, respectively. The measured radiation patterns follow similar trends to the full-wave simulation. However, there is a minor difference of beam direction from simulation and measured results, such as the difference for the beams at 9.6 GHz is only 5° between the predicted and measured ones. As mentioned earlier, this slight difference may occur for minor fabrication errors.

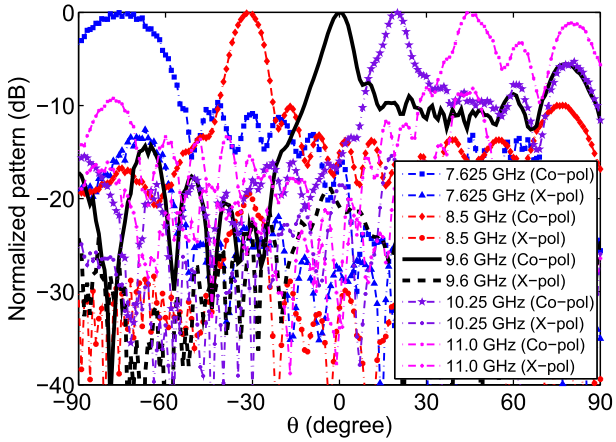

Fig. 16. Measured normalized radiation patterns (xz plane) of the SIW-based LWA2 prototype shown in Fig 15.

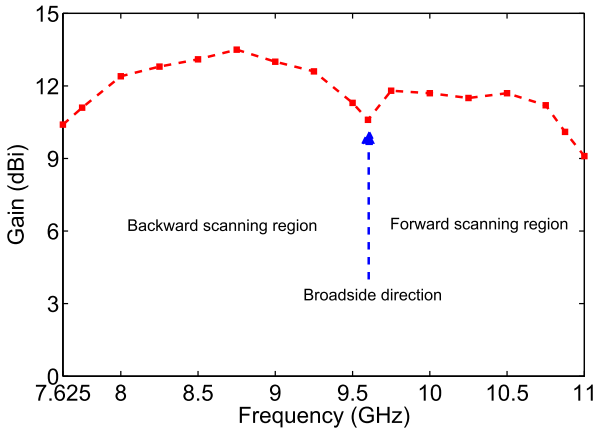

Fig. 17. Measured gain of the LWA2 prototype shown in Fig 15.

C. Measured Gain

Fig. 17 shows the measured gain of the LWA2 prototype. The gain was measured using a gain comparison method. The antenna has a measured peak gain of 13.5 dBi (at 8.75 GHz) and the measured gain is greater than 10.5 dBi between 7.75 and 10.75 GHz. The gains at 7.625 and 11 GHz are 10.4 and 9.1 dBi, respectively. The gain is low at higher frequency mainly due to poor impedance matching as well as high sidelobe level at this frequency point. However, from the gain curve, it can be seen that the proposed antenna has a stable gain within a wide scanning range.

VIII. Discussion

The main objective of this paper was to design an LWA using a unidirectional conventional periodic structure that has the ability to suppress completely the OSB at the broadside frequency and achieve continuous beam scanning though the broadside direction. However, while designing the antenna, we found some interesting features and those are summarized here. For the transverse slot antenna, the cross-polarization level is very high except in a very limited frequency range in the backward direction. Our original intention was to design a linearly polarized antenna by reducing the cross-polarization

TABLE II
COMPARISON BETWEEN THE SIW-BASED LWAS STUDIED IN THIS PAPER AND REFERENCE ANTENNAS

Antenna Structure	Type of Antenna	Broadside Gain	Gain Variation in Scan Range	Scanning Range
[18]	SIW	No beam	($\sim$) 6 dB	Forward only[1]
[19]	SIW	No beam	($\sim$) 6.5 dB	($\sim$) $+14^\circ$ to $+82^\circ$
[34]	HW microstrip	No beam	($\sim$) 8 dB	-59° to $+62^\circ$
[35]	HW microstrip	($\sim$) 1 dBi	($\sim$) 8 dB	-54° to $+49^\circ$
[36]	SIW	($\sim$) 11 dBi	($\sim$) 4 dB	-40° to $+35^\circ$
[37]	DIL	($\sim$) 14 dBi	6 dB	-65° to $+25^\circ$
[41]	SIW	No beam	($\sim$) 6.5 dB	($\sim$) $+5^\circ$ to $+64^\circ$
This work	SIW	10.60 dBi	4.4 dB	-74° to $+45^\circ$

SIW = substrate integrated waveguide; HW = Half-width; DIL = Dielectric image line.
[1]Scan range is not specified in the related publications. ($\sim$) is used for the data which has taken from figures through visual measurement.

when the beam crosses through broadside. We were able to meet our target by employing a new type of slot, the dual-slot approach. However, it is worth mentioning here that a slot is required for continuous beam scanning through broadside. We investigated an antenna design by removing slots from the design. It was found that when the slot is not present in the unit cell, the antenna is unable to scan through broadside. This happens because the structure does not radiate toward the broadside direction without a slot on the top plate. Moreover, an impedance mismatch and, hence, an OSB occur due to the reflection from the unit cell.

A comparison between the antennas is given in Table I. It can be seen that the cross-polarization level of LWA2 with $\theta_x = 80^\circ$ is much lower than for LWA1 and LWA2 with $\theta_x = 90^\circ$ when the beam points at broadside. It was found that LWA2 with $\theta_x = 80^\circ$ has a slightly wider beam scanning range. Comparisons between the fabricated LWA2 and reference antennas are given in Table II. For most reference antennas, they are either unable to radiate toward broadside or have a very poor radiation performance due to the restriction from the OSB. Some of the antennas listed in Table II are able to scan the beam through broadside, but the measured cross-polarization level is not reported. The dielectric image line LWA in [37] is able to scan the beam through broadside and the measured cross-polarization level for the broadside beam is approximately 20 dB lower than the co-polarization level. The measured cross-polarization level of the antenna proposed in the paper is ≤ -20.8 dB at the main beam direction for the broadside beam. Furthermore, the proposed antenna has a better performance than the reference antennas for most of the cases listed in Table II.

IX. CONCLUSION

The conventional SIW-based LWAs generally scan the main beam in the forward direction only. In this paper, we have presented a new class of SIW-based LWAs with high radiation efficiency which can scan the main beam continuously from backward to forward direction. For one SIW-based LWA design that used a transverse slot in each unit cell, it was found that when the main beam scans from backward to forward direction, the cross-polarization level increases significantly when the beam approaches broadside. Furthermore, the cross-polarization level remains high when the main beam scans in the forward direction. A technique to reduce the cross-polarization level throughout the beam scanning range was introduced and an additional SIW-based LWA was designed that had low cross-polarization. Finally, the antenna design was fabricated and the measured results agreed very well with the predicted ones. The measured results showed that 119° of continuous beam scanning can be achieved from the new SIW-based LWA.

REFERENCES

[1] D. R. Jackson, C. Caloz, and T. Itoh, "Leaky-wave antennas," *Proc. IEEE*, vol. 100, no. 7, pp. 2194–2206, Jul. 2012.
[2] D. K. Karmokar, K. P. Esselle, and S. G. Hay, "Fixed-frequency beam steering of microstrip leaky-wave antennas using binary switches," *IEEE Trans. Antennas Propag.*, vol. 64, no. 6, pp. 2146–2154, Jun. 2016.
[3] D. K. Karmokar, K. P. Esselle, and T. S. Bird, "Wideband microstrip leaky-wave antennas with two symmetrical side beams for simultaneous dual-beam scanning," *IEEE Trans. Antennas Propag.*, vol. 64, no. 4, pp. 1262–1269, Apr. 2016.
[4] T.-L. Chen, Y.-D. Lin, and J.-W. Sheen, "Microstrip-fed microstrip second higher order leaky-mode antenna," *IEEE Trans. Antennas Propag.*, vol. 49, no. 6, pp. 855–857, Jun. 2001.
[5] W. W. Hansen, "Radiating electromagnetic wave guide," U.S. Patent 2 402 622A, Nov. 26, 1940.
[6] L. O. Goldstone and A. A. Oliner, "Leaky-wave antennas I: Rectangular waveguides," *IRE Trans. Antennas Propag.*, vol. 7, no. 4, pp. 307–319, Oct. 1959.
[7] A. Alphones and M. Tsutsumi, "Leaky wave radiation from a periodically photoexcited semiconductor slab waveguide," *IEEE Trans. Microw. Theory Techn.*, vol. 43, no. 9, pp. 2435–2441, Sep. 1995.
[8] M. Garcia-Vigueras, J. L. Gomez-Tornero, G. Goussetis, A. R. Weily, and Y. J. Guo, "Enhancing frequency-scanning response of leaky-wave antennas using high-impedance surfaces," *IEEE Antennas Wireless Propag. Lett.*, vol. 10, pp. 7–10, 2011.
[9] M. Garcia-Vigueras, J. L. Gomez-Tornero, G. Goussetis, A. R. Weily, and Y. J. Guo, "1D-leaky wave antenna employing parallel-plate waveguide loaded with PRS and HIS," *IEEE Trans. Antennas Propag.*, vol. 59, no. 10, pp. 3687–3694, Oct. 2011.
[10] R. Guzman-Quiros, J. L. Gomez-Tornero, A. R. Weily, and Y. J. Guo, "Electronically steerable 1-D Fabry–Pérot leaky-wave antenna employing a tunable high impedance surface," *IEEE Trans. Antennas Propag.*, vol. 60, no. 11, pp. 5046–5055, Nov. 2012.
[11] W. Menzel, "A new travelling wave antenna in microstrip," in *Proc. 8th Eur. Microw. Conf.*, Sep. 1978, pp. 302–306.
[12] W. Menzel, "A new travelling wave antenna in microstrip," *Arch. Elektron. Uebertrag. Tech.*, vol. 33, no. 4, pp. 137–140, Apr. 1979.
[13] H. Ermert, "Guiding and radiation characteristics of planar waveguides," *IEE J. Microw., Opt. Acoust.*, vol. 3, no. 2, pp. 59–62, Mar. 1979.
[14] A. Oliner and K. Lee, "The nature of the leakage from higher modes on microstrip line," in *IEEE MTT-S Int. Microw. Symp. Dig.*, Jun. 1986, pp. 57–60.
[15] A. A. Oliner, "Leakage from higher modes on microstrip line with application to antennas," *Radio Sci.*, vol. 22, pp. 907–912, Nov. 1987.
[16] D. K. Karmokar and K. P. Esselle, "Periodic U-slot-loaded dual-band half-width microstrip leaky-wave antennas for forward and backward beam scanning," *IEEE Trans. Antennas Propag.*, vol. 63, no. 12, pp. 5372–5381, Dec. 2015.
[17] F. Xu, K. Wu, and X. Zhang, "Periodic leaky-wave antenna for millimeter wave applications based on substrate integrated waveguide," *IEEE Trans. Antennas Propag.*, vol. 58, no. 2, pp. 340–347, Feb. 2010.
[18] J. Liu, D. R. Jackson, and Y. Long, "Substrate integrated waveguide (SIW) leaky-wave antenna with transverse slots," *IEEE Trans. Antennas Propag.*, vol. 60, no. 1, pp. 20–29, Jan. 2012.
[19] Y. Mohtashami and J. Rashed-Mohassel, "A butterfly substrate integrated waveguide leaky-wave antenna," *IEEE Trans. Antennas Propag.*, vol. 62, no. 6, pp. 3384–3388, Jun. 2014.
[20] J. Macháč, P. Lorenz, M. Sağlam, C.-T. Bui, and W. Kraemer, "A substrate integrated waveguide leaky wave antenna radiating from a slot in the broad wall," in *IEEE MTT-S Int. Microw. Symp. Dig.*, May 2010, pp. 5–8.

[21] N. Nguyen-Trong, T. Kaufmann, and C. Fumeaux, "A wideband omnidirectional horizontally polarized traveling-wave antenna based on half-mode substrate integrated waveguide," *IEEE Antennas Wireless Propag. Lett.*, vol. 12, pp. 682–685, 2013.
[22] D. K. Karmokar, Y. J. Guo, P.-Y. Qin, K. P. Esselle, and T. S. Bird, "Forward and backward beam-scanning tri-band leaky-wave antenna," *IEEE Antennas Wireless Propag. Lett.*, vol. 16, pp. 1891–1894, 2017.
[23] D. K. Karmokar, K. P. Esselle, and T. S. Bird, "An array of half-width microstrip leaky-wave antennas radiating on boresight," *IEEE Antennas Wireless Propag. Lett.*, vol. 14, pp. 112–114, 2015.
[24] A. J. Martinez-Ros, J. L. Gómez-Tornero, and G. Goussetis, "Broadside radiation from radial arrays of substrate integrated leaky-wave antennas," in *Proc. 6th Eur. Conf. Antennas Propag. (EuCAP)*, Mar. 2012, pp. 252–254.
[25] D. K. Karmokar, K. P. Esselle, S. G. Hay, T. S. Bird, and M. Heimlich, "A simple single-feed array of uniform half-width microstrip leaky-wave antennas for boresight radiation," in *Proc. Int. Symp. Antennas Propag. (ISAP)*, Nov. 2015, pp. 1–3.
[26] A. J. Martinez-Ros, J. L. Gómez-Tornero, and G. Goussetis, "Pencil beam radiation pattern from a single-layer substrate-integrated waveguide leaky-wave antenna with simple feeding," *IET Microw., Antennas Propag.*, vol. 9, no. 1, pp. 24–30, 2015.
[27] L. Liu, C. Caloz, and T. Itoh, "Dominant mode leaky-wave antenna with backfire-to-endfire scanning capability," *Electron. Lett.*, vol. 38, no. 23, pp. 1414–1416, Nov. 2002.
[28] Nasimuddin, Z. N. Chen, and X. Qing, "Multilayered composite right/left-handed leaky-wave antenna with consistent gain," *IEEE Trans. Antennas Propag.*, vol. 60, no. 11, pp. 5056–5062, Nov. 2012.
[29] C. Jin and A. Alphones, "Leaky-wave radiation behavior from a double periodic composite right/left-handed substrate integrated waveguide," *IEEE Trans. Antennas Propag.*, vol. 60, no. 4, pp. 1727–1735, Apr. 2012.
[30] A. P. Saghati, M. M. Mirsalehi, and M. H. Neshati, "A HMSIW circularly polarized leaky-wave antenna with backward, broadside, and forward radiation," *IEEE Antennas Wireless Propag. Lett.*, vol. 13, pp. 451–454, 2014.
[31] N. Nasimuddin, Z. N. Chen, and X. Qing, "Substrate integrated metamaterial-based leaky-wave antenna with improved boresight radiation bandwidth," *IEEE Trans. Antennas Propag.*, vol. 61, no. 7, pp. 3451–3457, Jul. 2013.
[32] P. Burghignoli, G. Lovat, and D. R. Jackson, "Analysis and optimization of leaky-wave radiation at broadside from a class of 1-D periodic structures," *IEEE Trans. Antennas Propag.*, vol. 54, no. 9, pp. 2593–2604, Sep. 2006.
[33] S. K. Podilchak, A. P. Freundorfer, and Y. M. M. Antar, "Broadside radiation from a planar 2-D leaky-wave antenna by practical surface-wave launching," *IEEE Antennas Wireless Propag. Lett.*, vol. 7, pp. 517–520, 2008.
[34] Y. Li, Q. Xue, E. K. N. Yung, and Y. Long, "The periodic half-width microstrip leaky-wave antenna with a backward to forward scanning capability," *IEEE Trans. Antennas Propag.*, vol. 58, no. 3, pp. 963–966, Mar. 2010.
[35] Y. Li, Q. Xue, H.-Z. Tan, and Y. Long, "The half-width microstrip leaky wave antenna with the periodic short circuits," *IEEE Trans. Antennas Propag.*, vol. 59, no. 9, pp. 3421–3423, Sep. 2011.
[36] Y. L. Lyu *et al.*, "Leaky-wave antennas based on noncutoff substrate integrated waveguide supporting beam scanning from backward to forward," *IEEE Trans. Antennas Propag.*, vol. 64, no. 6, pp. 2155–2164, Jun. 2016.
[37] C. S. Prasad and A. Biswas, "Dielectric image line-based leaky-wave antenna for wide range of beam scanning through broadside," *IEEE Trans. Antennas Propag.*, vol. 65, no. 8, pp. 4311–4315, Aug. 2017.
[38] A. A. Oliner and D. R. Jackson, "Leaky-wave antennas," in *Antenna Engineering Handbook*, J. Volakis, Ed. New York, NY, USA: McGraw-Hill, 2007, ch. 11.
[39] S. Paulotto, P. Baccarelli, F. Frezza, and D. R. Jackson, "A novel technique for open-stopband suppression in 1-D periodic printed leaky-wave antennas," *IEEE Trans. Antennas. Propag.*, vol. 57, no. 7, pp. 1894–1906, Jul. 2009.
[40] J. T. Williams, P. Baccarelli, S. Paulotto, and D. R. Jackson, "1-D combline leaky-wave antenna with the open-stopband suppressed: Design considerations and comparisons with measurements," *IEEE Trans. Antennas Propag.*, vol. 61, no. 9, pp. 4484–4492, Sep. 2013.
[41] A. J. Martinez-Ros, J. L. Gomez-Tornero, and G. Goussetis, "Planar leaky-wave antenna with flexible control of the complex propagation constant," *IEEE Trans. Antennas Propag.*, vol. 60, no. 3, pp. 1625–1630, Mar. 2012.

Debabrata K. Karmokar (S'12–M'15) was born in Satkhira, Bangladesh. He received the B.Sc. degree in electrical and electronic engineering (EEE) from the Khulna University of Engineering and Technology (KUET), Khulna, Bangladesh, in 2007, and the Ph.D. degree in electronic engineering from Macquarie University, Sydney, NSW, Australia, in 2015.

He was an Assistant Professor and a Member of Consultancy, Research, and Testing Services, Department of EEE, KUET, also an Assistant Director of Students' Welfare of the University. He was a Secretary of the IEEE Student Branch, Macquarie University, where he was a Research Assistant with the Department of Engineering from 2015 to 2016. He is currently a Post-Doctoral Research Associate with the Global Big Data Technologies Centre, Faculty of Engineering and Information Technology, University of Technology Sydney, Ultimo, NSW, Australia.

Dr. Karmokar was a recipient of the District Council Scholarship from Satkhira District Council, Bangladesh, the Technical Scholarship from KUET, the Commonwealth-Funded International Postgraduate Research Scholarship, the International Macquarie University Research Excellence Scholarship from Macquarie University, the OCE Ph.D. Scholarship from the Commonwealth Scientific and Industrial Research Organisation, ICT Centre, Marsfield, NSW, and the First Prize in the Poster Competition at the Engineering Symposium 2015, Macquarie University. He is serving as a reviewer for several journals, including the IEEE TRANSACTIONS ON ANTENNAS AND PROPAGATION, IEEE ANTENNAS AND WIRELESS PROPAGATION LETTERS, IEEE ANTENNAS AND PROPAGATION MAGAZINE, the IEEE ACCESS and the *IET Microwaves, Antennas and Propagation*.

Y. Jay Guo (F'14) received the bachelor's and master's degrees from Xidian University, Xi'an, China, in 1982 and 1984, respectively, and the Ph.D. degree from Xi'an Jiaotong University, Xi'an, in 1987.

He held various senior leadership positions in Fujitsu, U.K., Siemens, U.K., and NEC, U.K. In 2014, he was a Research Director with Commonwealth Scientific and Industrial Research Organisation, Marsfield, NSW, Australia, for over nine years, and managing a number of ICT research portfolios. He is currently the Director of Global Big Data Technologies Centre, Faculty of Engineering and Information Technology, University of Technology Sydney, Ultimo, NSW, Australia, and a Distinguished Professor with the University of Technology Sydney, Ultimo, NSW. His current research interests include reconfigurable antennas, conformal and wideband arrays, metamaterial, millimeter-wave and terahertz communications, and sensing systems.

Dr. Jay is a Fellow of the Australian Academy of Engineering and Technology and the Institution of Electrical Technology, and a member of the College of Experts of Australian Research Council. He has chaired numerous international conferences. He is the International Advisory Committee Chair of the IEEE VTC2017, the General Chair of ISAP2015, iWAT2014, and WPMC'2014, and the TPC Chair of the 2010 IEEE WCNC and the 2012 and 2007 IEEE ISCIT. He was a recipient of a number of prestigious Australian National Awards, and was named one of the most influential engineers in Australia in 2014 and 2015. He serves as a Guest Editor for special issues on *Antennas for Satellite Communications* and *Antennas and Propagation Aspects of 60–90GHz Wireless Communications*, both in the IEEE TRANSACTIONS ON ANTENNAS AND PROPAGATION, Special Issue on *Communications Challenges and Dynamics for Unmanned Autonomous Vehicles*, in the IEEE JOURNAL ON SELECTED AREAS IN COMMUNICATIONS, and Special Issue on *5G for Mission Critical Machine Communications*, in IEEENETWORK MAGAZINE.

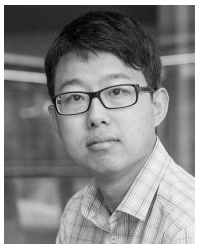

Pei-Yuan Qin (M'13) was born in Liaoning, China, in 1983. He received the bachelor's degree in electronic engineering from Xidian University, Xi'an, China, in 2006, and the joint Ph.D. degree in electromagnetic fields and microwave technology from Xidian University and Macquarie University, Sydney, NSW, Australia, in 2012.

From 2012 to 2015, he was a Post-Doctoral Research Fellow with Commonwealth Scientific and Industrial Research Organisation. From 2015 to 2016, he was a Chancellor's Post-Doctoral Research Fellow/Lecturer with the University of Technology Sydney, Ultimo, NSW, where he has been a Senior Lecturer since 2017. His current research interests include reconfigurable antennas, phase shifters, reconfigurable reflect arrays, and multi-in multi-out communications.

Dr. Qin was a recipient of the Australia Research Council Discovery Early Career Researcher Award, the International Macquarie University Research Excellence Scholarship, the Vice Chancellor's Commendation for academic excellence by Macquarie University, and 2016 Computer Simulation Technology University Publication Award for one of his papers. Since 2017, he has been an Associate Editor of IEEE ANTENNAS AND WIRELESS PROPAGATION LETTERS.

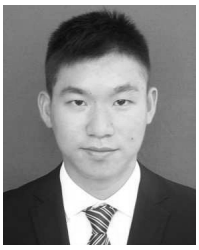

Shu-Lin Chen (S'16) was born in Hubei, China. He received the B.S. degree in electrical engineering from Fuzhou University, Fuzhou, China, in 2012, and the M.S. degree in electromagnetic field and microwave technology from Xiamen University, Xiamen, China, in 2015. He is currently pursuing the Ph.D. degree in engineering with the Global Big Data Technologies Centre, University of Technology Sydney, Sydney, NSW, Australia.

He authored or co-authored over 15 journal and conference papers. His current research interests include reconfigurable antennas, leaky wave antennas, millimeter-wave antennas, and adaptive array processing.

Mr. Chen was a finalist of the ISAP 2017 Student Paper Competition, and his paper was listed as an Honorary Mention in APS-URSI 2017.

Trevor S. Bird (S'71–M'76–SM'85–F'97–LF'15) received the B.App.Sc., M.App.Sc., and Ph.D. degrees from the University of Melbourne, Melbourne, VIC, Australia, in 1971, 1973, and 1977, respectively.

He was a Post-Doctoral Research Fellow with the Queen Mary College, University of London, London, U.K. He was a Lecturer with the Department of Electrical Engineering, James Cook University, Townsville, QLD, Australia. In 1983, he joined the Commonwealth Scientific and Industrial Research Organization, Sydney, NSW, Australia, where he held several positions, including the Chief Scientist of the ICT Centre, Marsfield, NSW. From 1982 to 1983, he was a Consultant with Plessey Radar, London. He is currently the Principal of Antengenuity, a specialist consulting firm, a Distinguished Visiting Professor with the University of Technology Sydney, Ultimo, NSW, and an Adjunct Professor with Macquarie University, North Ryde, NSW.

Dr. Bird is a Fellow of the Australian Academy of Technological and Engineering Sciences, the Institution of Electrical Technology (IET), Queens College, University of Melbourne, and an Honorary Fellow of the Institution of Engineers, Australia. He was a member of the New South Wales Section Committee from 1995 to 2005, the Administrative Committee of the IEEE Antennas and Propagation Society from 2003 to 2005, the College of Experts of the Australian Research Council from 2006 to 2007, and the Technical Committee of numerous conferences, including JINA, ICAP, AP2000, IRMMW-THz, and the URSI Electromagnetic Theory Symposium. He was a Distinguished Lecturer for the IEEE Antennas and Propagation Society from 1997 to 1999, the Chair of the New South Wales Joint AP/MTT Chapter from 1995 to 1998, and again in 2003, the Chairman of the 2000 Asia Pacific Microwave Conference, and a Vice-Chair and the Chair of the Section from 1999 to 2000 and from 2001 to 2002, respectively. He was a recipient of the John Madsen Medal of the Institution of Engineers, Australia, on four occasions for the best paper published annually in the *Journal of Electrical and Electronic Engineering*, the CSIRO Medals for achievement in 1990, 1998, and 2011, the IEEE Third Millennium Medal for outstanding contributions to the IEEE New South Wales Section in 2000, several project awards from the Society of Satellite Professionals International (New York) in 2004, the Engineers Australia in 2001, and the Communications Research Laboratory, Japan, in 2000, the Centenary Medal for service to Australian society in telecommunications, the M.A. Sargent Medal in 2012 by Engineers Australia for sustained contributions to electrical engineering, and the James R. James Lifetime Achievement Award of IET in 2016 for outstanding contributions to the field of antennas and propagation. He was a co-recipient of the H.A. Wheeler Applications Prize Paper Award of the IEEE Antennas and Propagation Society in 2001. He was also named Professional Engineer of the Year by the Sydney Division, Engineers Australia in 2003. Since 2006, his biography has been listed in Who's Who in Australia. He was an Associate Editor of the IEEE TRANSACTIONS ON ANTENNAS AND PROPAGATION from 2001 to 2004, the Editor-in-Chief of the IEEE TRANSACTIONS ON ANTENNAS AND PROPAGATION from 2004 to 2010, and the President of the Society in 2013.